IV International Conference on Particle-based Methods – Fundamentals and Applications
PARTICLES 2015
E. Oñate, M. Bischoff, D.R.J. Owen, P. Wriggers & T. Zohdi (Eds)

NUMERICAL MODELING OF METAL CUTTING PROCESSES USING THE PARTICLE FINITE ELEMENT METHOD (PFEM) AND A PHYSICALLY BASED PLASTICITY MODEL

RODRÍGUEZ J.M. [1], JONSÉN, P. [2] AND SVOBODA, A.[3]

[1] Division of Mechanics of Solid Materials
Department of Engineering Sciences and Mathematics. Lulea University of Technology
E-mail rodjua@ltu.se
[2] Division of Mechanics of Solid Materials
Department of Engineering Sciences and Mathematics. Lulea University of Technology
E-mail par.Jonsen@ltu.se
[3] Division of Mechanics of Solid Materials
Department of Engineering Sciences and Mathematics. Lulea University of Technology
E-mail ales.svoboda@ltu.se

Key words: Particle Finite Element Method, Dislocation density constitutive models, Metal cutting.

Abstract. Metal cutting is one of the most common metal shaping processes. Specified geometrical and surface properties are obtained by break-up of material and removal by a cutting edge into a chip. The chip formation is associated with large strain, high strain rate and locally high temperature due to adiabatic heating which make the modeling of cutting processes difficult. Furthermore, dissipative plastic and friction work generate high local temperatures. These phenomena together with numerical complications make modeling of metal cutting difficult. Material models, which are crucial in metal cutting simulations, are usually calibrated based on data from material testing. Nevertheless, the magnitude of strain and strain rate involved in metal cutting are several orders higher than those generated from conventional material testing. Therefore, a highly desirable feature is a material model that can be extrapolated outside the calibration range. In this study a physically based plasticity model based on dislocation density and vacancy concentration is used to simulate orthogonal metal cutting of AISI 316L. The material model is implemented into an in-house Particle Finite Element Method software. Numerical simulations are in agreement with experimental results, but also with previous results obtained with the finite element method.

1 INTRODUCTION

Cutting tool designs and cutting process parameters may be optimized by experimental measurements or by numerical analysis. In deformation zones in front of the tool and beneath the cutting edge, the material is deformed plastically by simultaneous action of large compressive and shearing stresses. The friction forces and dissipative plastic work generate high temperatures. This makes direct observation in the cutting zone during machining difficult.

In this study, the particle finite element method (PFEM) using a physical based dislocation density model is compared with a set of numerical simulations carried out using the finite element method (FEM).

2 THE PARTICLE FINITE ELEMENT METHOD

Let us consider a domain containing a fluid. This domain is characterized by a set of points, hereafter called *particles*. The particles contain all the information for defining the geometry and the material and mechanical properties of the underlying domain.
Summary of the steps
The PFEM is conceived for the solution of fluid-dynamics problems using a Lagrangian approach based on the formulation of the Navier–Stokes equations in material coordinates[3]. The PFEM, typically, consists of the following steps
1. Fill the fluid domain with a set of points referred to as 'particles'. The accuracy of the numerical solution is clearly dependent on the considered number of particles.
2. Generate a finite element mesh using the particles as nodes. This is achieved using a Delaunay triangulation.
3. Identify the external boundaries to impose the boundary conditions and to compute the domain integrals.
4. Solve the non-linear Lagrangian form of the governing equations finding velocity and pressure at every node of the mesh.
5. Update the particle positions using the computed values of velocity and pressure.
6. Go back to step 2 and repeat for the next time step.
In this solution scheme, not only is the numerical solution of the equations critical from the computational point of view, but so are the generation of a new mesh and the identification of the boundaries. To this purpose a Delaunay triangulation scheme is adopted together with the boundary identification method presented in the following section.
Identification of the boundaries
In a Lagrangian framework the external boundary and the reference volume are defined by the position of the material particles. Every time the mesh is regenerated, the particles belonging to the boundary may change and the new boundary nodes (and therefore the particles) have to be identified. The Delaunay triangulation generates the convex hull of the set of particles. Moreover, the convex hull may not be conformal with the external boundaries. A possibility to overcome this problem is to correct the generated mesh using the so-called **α**-shape method to remove the unnecessary triangles from the mesh using a criterion based on the mesh distortion. The **α**-shape method can also be used for the identification of the fluid particles which separate from the rest of the domain.

2.1 The particle finite element method in the numerical simulation of metal cutting processes

The standard PFEM presents some weaknesses when applied in orthogonal cutting simulation. For example, the external surface generated using **α**-shape may affect the mass conservation, the chip shape and sometimes generates an unphysical welding of the workpiece and the chip.
To deal with this problem, in this work we propose the use of a constrained Delaunay algorithm. Furthermore, addition and remotion of particles are the principal tools, which we employ for sidestepping the difficulties, associated with deformation-induced element distortion, and for resolving the different scales of the solution.

In the numerical simulation of metal cutting process, despite the continuous Delaunay triangulation, elements arise with unacceptable aspect ratios; for this reason, the mesh is also subjected to laplacian smoothing. Laplacian smoothing is an algorithm to smooth a mesh. For each node in a mesh, a new position is chosen based on the position of neighbors and the node is moved there. In the case that a mesh is topologically a rectangular grid then this operation produces the Laplacian of the mesh.

3 PHYSICAL BASED MODELS

Physical based models are models where the physical mechanisms are underlying the deformation in contrast to empirical models which are of a more curve-fitting nature. However, due to the need for averaging and also limited knowledge about some of the relations making up the model, physical based models need also be calibrated. Two different types of physical based models exist. One option is to explicitly include variables from physics as internal state variables. The other possibility is to determine the format of the constitutive equation based on knowledge about the physical mechanisms causing the deformation. The latter is a so-called "model- based-phenomenology" Some advantages of physical based models is the possibility to link effects from other scales, e.g. via parameters for grain size or models for microstructure evolution that extends the model validity to a larger domain. This may extrapolated the validity of the model outside their range of calibration. This requires that the physical mechanisms implemented in the models still dominate the deformation in the extended range.

The dislocation density model consider dislocation glide and climb processes contributions to the plastic straining. The yield limit in this approach is separated into two components according to

$$\sigma_y = \sigma_G + \sigma^* \tag{1}$$

σ_G and σ^* are the long-range athermal component and the short-range contributions to the flow stress, respectively. The first component σ_G, is the stress needed to overcome the long-range interactions lattice distortions due to the dislocation substructure. The second component, σ^*, is the stress needed for the dislocation to pass through the lattice and to pass short-range obstacles. Thermal vibrations will then also assist the dislocation when passing an obstacle. The long-range stress component is commonly written as;

$$\sigma_G = m\alpha Gb\sqrt{\rho_i} \tag{2}$$

where m is the Taylor orientation factor, α is a proportionality factor, G is the temperature dependent shear modulus, b is the magnitude of Burgers vector and ρ_i is the immobile dislocation density. The short-range stress components may be written as,

$$\sigma^* = \hat{\tau} G \left\{ 1 - \left[\frac{kT}{\Delta F b^3 G} \ln\left(\frac{\dot{\bar{\varepsilon}}_{ref}}{\dot{\bar{\varepsilon}}^p} \right) \right]^{\frac{1}{q}} \right\}^{\frac{1}{p}} \tag{3}$$

where ΔF denote the required free energy needed to overcome the lattice resistance or obstacles without assistance from external stress, τ denote the athermal flow strength required to move the dislocation past barriers without assistance of thermal energy, $\dot{\bar{\varepsilon}}_{ref}$ denote the reference strain rate. The exponent p and q characterize the barrier profiles and usually have values between $0 \le p \le 1$ and $0 \le q \le 2$ respectively.

3.1 Structure evolution

The evolution of the structure is considered to consist of a hardening and a recovery process. The used model assumes that the mobile dislocation density is stress and strain independent and much smaller than the immobile ones. Hence the evolution equation is written;

$$\dot{\rho}_i = \dot{\rho}_i^{(+)} - \dot{\rho}_i^{(-)} \tag{4}$$

where index i denotes the immobile dislocations. The increase in immobile dislocation density is assumed to be related to the plastic strain rate and may therefore be written according to

$$\dot{\rho}_i^{(+)} = \frac{m}{b} \frac{1}{\lambda} \dot{\bar{\varepsilon}}^p \tag{5}$$

where λ denote the mean free path which is a function of the size of the grains and the dislocation sub-cell diameter. The recovery may occur by dislocation glide and/or climb. The former is described by

$$\dot{\rho}_i^{(-)} = \Omega \rho_i \dot{\bar{\varepsilon}}^p \tag{6}$$

where Ω is a recovery function which depends on the temperature and strain rate. Recovery by climb is describe by

$$\dot{\rho}_i^{(-)} = 2 c_\gamma \frac{D_v}{c_v^{eq}} \frac{G b^3}{kT} (\rho_i^2 - \rho_{eq}^2) c_v \tag{7}$$

where c_v is the vacancy fraction, c_v^{eq} is the thermal equilibrium vacancy concentration, D_v is the diffusivity and c_γ is a calibration parameter. More details are found in (Lindgren et al).

4 NUMERICAL MODELING OF METAL CUTTING PROCESSES USING PFEM AND A PHYSICAL BASED CONSTITUTIVE MODEL

The orthogonal cutting process has been analyzed utilizing an in-house particle finite element method code. This software is based on a Lagrangian formulation combined with an implicit time integration scheme. A staggered method for coupled transient mechanical and heat transfer analysis is used. A mixed displacement-pressure linear finite element with one integration point was used. A continuous Delaunay triangularization of the particle in its updated configuration facilitates the analysis facing large excessive deformations and shear localization. The insertion of particles at different deformation zones occurs through a plastic power error estimator. The physical based material model was implemented inside the code as a new material model. This was based on a thermo-elasto-plastic model with isotropic hardening using a multiplicative decomposition plasticity formulation which takes account high strain rates.

An orthogonal cutting operation was employed to mimic 2D plain strain conditions. The depth of cut, used for all the test cases, was equal to 3mm. The dimension of the workpiece was 8*1.6 mm. A horizontal velocity corresponding to the cutting speed was applied to the particles at the right side of the tool. The particles along the bottom and the left sides of the workpiece were fixed. Cutting data used for the numerical simulations are the same used in Svoboda et al (2010).

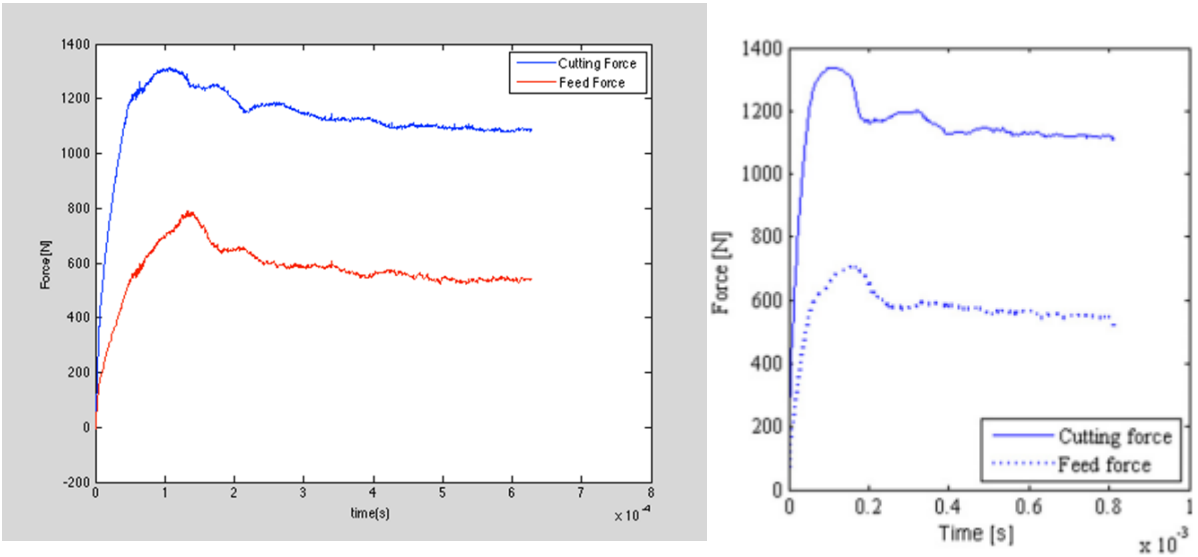

(a) (b)

Figure 1: Comparison of cutting and feed force PFEM-FEM. In (a) results predicted by PFEM and in (b) results predicted by FEM.

The loading histories of simulated forces (see figure above), were evaluated at the tool chip interface. Figure 1 on the left presents the results using PFEM and the figure on the right present the results using FEM (Svoboda et al 2010). The force time curves are very similar for both numerical simulations. Average values of the computed forces in the steady state region are compared with experimental results and numerical results obtained using FEM presented in Svoboda et al (2010) in the following table.
The table 1 shows that the cutting force was overestimated in all tests by about 15%. Meanwhile, the feed force was underestimated by about 5%. The results presented in the table above were compared with the results in Svoboda et al (2010), showing that PFEM is able to predict results to those obtained using (FEM). Literature overview (Lindgren, 2009) show that in the industrial production of nominally identical cutting tool as well as variations in material properties of nominally the same material can cause variations around the 10% in forces.

Table 1: Simulated cutting and feed forces

Table 4. Measured and simulated cutting forces.

Test	Measured		Simulated JC				Simulated DD			
no	F_c (N)	F_f (N)	F_c (N)	e (%)	F_f (N)	e (%)	F_c (N)	e (%)	F_f (N)	e (%)
1	446	437	425	−4.7	350	−19.9	485	8.7	400	−8.5
2	960	592	1065	10.9	515	−13.0	1100	14.6	545	−7.9
3	442	439	440	−0.5	355	−19.4	480	8.6	390	−11.2
4	929	560	1050	13.0	510	−8.9	1075	15.7	530	−5.4

Test no	Fc(N)	E(%)	Ff(N)	E(%)
1	513.6	15.1	427.6	-2,15
2	1100	14.5	557	-5,91
3	507	14.7	411	-6,38
4	1094	17.7	549	-1,96

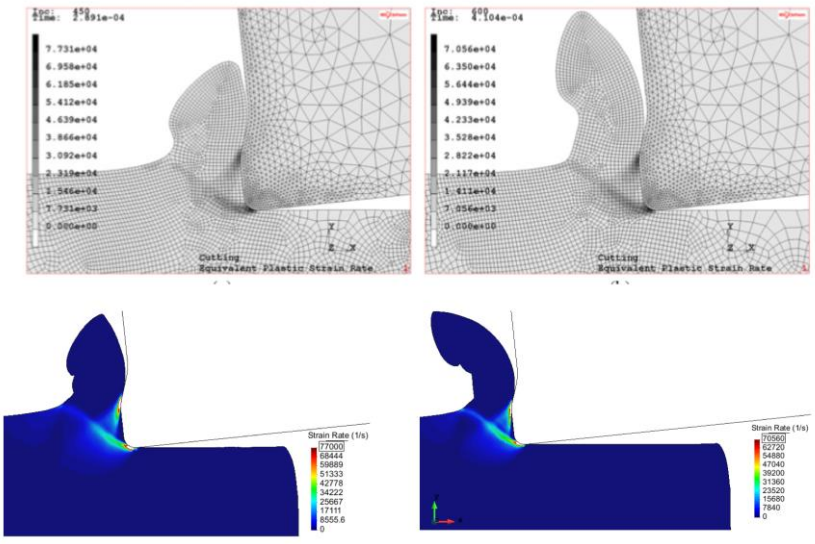

Figure 2: Effective plastic strain rate. FEM and FEM

Figure 2 illustrates distribution of plastic strain rates in the primary and the secondary shear zones. A comparison of the predicted chip shape using PFEM (below) and FEM (above) shows that the numerical strategies predict similar chip shapes, although the chip tool contact length predicted by PFEM a little lower than FEM.

CONCLUSIONS

In this work a dislocation density model have been used together with PFEM to virtually reproduce orthogonal cutting of AISI 316L steel. Numerical results obtained using PFEM have been compared with both experimental results and numerical results. The PFEM based numerical model can also predict similar strain rate distribution and chip shape as the FEM model. Also, the numerical model developed within this work is in agreement with experimental results and can predict forces near the wanted precision.

REFERENCES

[1] Svoboda A, Wedberg D and Lindgren L-E 2010 Simulation of metal cutting using a physically-based plasticity model. Modelling Simul. Mater. Sci. Eng. 18 1–19Idelsohn, S.R. and Oñate, E. Finite element and finite volumes. Two good friends. *Int. J. Num. Meth. Engng* (1994) **37**:3323-3341.

[2] Rodriguez, J. M. 2014. Numerical modeling of metal cutting processes using the Particle Finite Element Method (PFEM). http://hdl.handle.net/10803/145692

[3] S. R. Idelsohn, E. Oñate, and F. D. Pin, "The particle finite element method: a powerful tool to solve incompressible flows with free-surfaces and breaking waves," International Journal for Numerical Methods in Engineering, vol. 61, pp. 964-989, 2004